Journal of Hazardous Materials 217–218 (2012) 293–300

Contents lists available at SciVerse ScienceDirect

Journal of Hazardous Materials

journal homepage: www.elsevier.com/locate/jhazmat

Evaluation of three reagent dosing strategies in a photo-Fenton process for the decolorization of azo dye mixtures

D. Prato-Garcia, Germán Buitrón*

Laboratory for Research on Advanced Processes for Water Treatment, Instituto de Ingeniería, Unidad Académica Juriquilla, Universidad Nacional Autónoma de México, Blvd. Juriquilla 3001, Querétaro 76230, Mexico

ARTICLE INFO

Article history:
Received 14 November 2011
Received in revised form 22 February 2012
Accepted 10 March 2012
Available online 22 March 2012

Keywords:
Azo
Biodegradability
Photo-Fenton
Reagent injection
Toxicity

ABSTRACT

Three reagent dosing strategies used in the solar photo-assisted decolorization of a mixture of sulfonated dyes consisting of acid blue 113, acid orange 7 and acid red 151 were evaluated. Results demonstrated that the dosing strategy influenced both reagent consumption and the biodegradability and toxicity of the effluent. In one strategy (E_1), the Fenton's reactants were dosed in a punctual mode, while in the other two strategies (E_2 an E_3), the reactants were dosed continuously. In the E_2 strategy the reactants were dosed by varying the duration of the injection time. In the E_3 strategy, the reactants were dosed during 60 min at a constant rate, but with different concentrations. All cases showed that feeding the reactor between 40% and 60% of the maximal dose was sufficient to decolorize more than 90% of the mixture of azo dyes. The E_1 strategy was less effective for aromatic content reduction. Conversely, the continuous addition of the reagents (E_2 and E_3 strategies) improved the aromatic content removal. E_3 strategy was substantially more appropriate than E_1 strategy due to improved the effluent quality in two key areas: toxicity and biodegradability.

1. Introduction

Advanced oxidation processes (AOPs) have been used extensively for the degradation of a broad range of contaminants [1–4]. Nevertheless, AOPs have rarely been applied to the treatment of textile mill effluents because of their high operative costs and the presence of dye additives, impurities that can significantly reduce their performance [1,2,4–8]. Although the mineralization of dyes by AOPs is generally expensive, combining AOPs with biological processes may lead to a significant reduction in operative costs [1,4–11]. AOPs are generally designed to transform recalcitrant compounds up to more biodegradable by-products that can be degraded efficiently through aerobic processes [1,12–15]. Recently, the degradation of compounds formerly considered recalcitrant has been made possible through the use of photo-Fenton processes coupled with aerobic systems [1,10–15].

As indicated by [1,10,16] the reagent dose (Fe^{2+}–H_2O_2) may significantly affect the performance of a coupled system. A low initial ratio of reagents ($[Fe^{2+}]/[H_2O_2] < 1$) favors the formation of $HO^{\bullet}{}_2$ (Eq. (2)), a less powerful oxidant than the $HO^{\bullet}$ radical [1–4,16]. On the contrary, a high initial ratio of reagents ($[Fe^{2+}]/[H_2O_2] > 2$) results in a rapid depletion of $HO^{\bullet}$ (Eq. (3)) due to its reaction with Fe^{2+} (ten times faster than between $HO^{\bullet}$ and H_2O_2). Furthermore, the punctual injection of reactants may lead to a sharply production of $HO^{\bullet}$ radicals due to high localized concentrations of reagents [17–20]. Unfortunately, this drives to undesirable reactions (Eqs. (2)–(4)) which can consume $HO^{\bullet}$ radicals, reducing the oxidative capacity of the reactants over time [17–20]. It has been observed that a sub-stoichiometric dose of reagents leads to the formation of molecules that are potentially or even more toxic and recalcitrant than the parent compound [10,15]. Then, the dosing strategy of reagents could play a major role in the performance of a coupled chemical–biological system, having a significant relationship between the concentration of the reagent and the dosing strategy used in such parameters as cost, carbon removal, biodegradability and toxicity [16–19].

$$Fe^{2+} + H_2O_2 \rightarrow Fe^{3+} + HO^{\bullet} + OH^{-} \quad k = 53\text{–}76\,M^{-1}\,s^{-1} \tag{1}$$

$$HO^{\bullet} + H_2O_2 \rightarrow HO_2{}^{\bullet} + H_2O \quad k = 1.7\text{–}4.5 \times 10^{7}\,M^{-1}\,s^{-1} \tag{2}$$

$$HO^{\bullet} + Fe^{2+} \rightarrow Fe^{3+} + OH^{-} \quad k = 2.6\text{–}5.8\,M^{-1}\,s^{-1} \tag{3}$$

$$2HO^{\bullet} \rightarrow H_2O_2 \quad k = 5\text{–}8 \times 10^{9}\,M^{-1}\,s^{-1} \tag{4}$$

Despite their importance, the development of strategies for the dosing of reagents has gone virtually unnoticed [7–14]. As mentioned by several authors [17–19], the stepwise addition of peroxide would reduce the impact of adverse reactions (Eqs. (2)–(4)). The observed results evidenced an important improvement

* Corresponding author.
E-mail addresses: gbuitronm@iingen.unam.mx, gbuitronm@ii.unam.mx (G. Buitrón).

0304-3894/$ – see front matter © 2012 Elsevier B.V. All rights reserved.
doi:10.1016/j.jhazmat.2012.03.036

in process such parameters as carbon removal, degradation rate and peroxide efficiency [17–19]. Although stepwise addition of reagents may allow successful mineralization of recalcitrant compounds, the issues associated to reagents consumption could be considered as a main disadvantage [15,17–21]. On the other hand, the continuous addition of the reagents positively affects carbon removal and the degradation rate of the azo dye acid orange II (AO7). Nevertheless, both the single-step and continuous addition of the reagents allows 100% decolorization [22]. It is important to point out that the stepwise addition of the reagents seems to have a marginal [17,18,23], or even negative effect [24], on the mineralization of recalcitrant compounds.

In general, toxic wastewaters has been proven to lose its toxicity upon treatment by AOP before total mineralization has been achieved, therefore the improvement of the biodegradability instead of its mineralization may allow a cost reduction during the treatment of xenobiotic compounds [1,4,9–13,15]. In a coupled system (photo-Fenton + aerobic), it would be necessary to determine the best operating conditions for carrying out pre-treatment, so as to ensure the efficient performance of the aerobic process. In this study we focused on developing a strategy to reduce the adverse reactions that can occur in the Fenton process by regulating the dosage of reagents during the photo-degradation of a synthetic azo dye mixture. The aim was to assess both the concentration effect of the reagent (Fe^{2+}–H_2O_2) and the dosing strategy used on the toxicity and biodegradability of the pre-treated effluent. To do so, three reagent-dosing strategies used in the solar photo decolorization of a mixture of acid blue 113, acid orange 7 and acid red 151 were evaluated.

2. Experimental

2.1. Reagents

The selection of the best strategy for the dosage of the Fenton's reagents was tested on a mixture of three azo dyes: acid red 151 (AR151, $C_{22}H_{15}N_4NaO_4S$, C.I. 26,900, λ_{max}: 514 nm), acid orange 7 (AO7, $C_{16}H_{11}N_2NaO_4S$, C.I: 15510, λ_{max}: 484 nm) and acid blue 113 (AB113, C.I. 26360, dye content 50%, Sigma–Aldrich) at acidic pH (2.8 ± 0.2). AR151 and AO7 were commercial grade (Clariant, Mexico). Other reagents used were: $FeSO_4{\cdot}7H_2O$ (Sigma Aldrich, 97%), H_2O_2 (50%, w/v, Reproquifin), NH_4VO_3 (Sigma Aldrich, 99%), H_2SO_4 (Sigma Aldrich, 96%), NaOH (Sigma Aldrich, 96%) and phenol (C_6H_6O, Sigma Aldrich, 99%). The dye stock solutions (1 g/L) and reagents used in the analytical determinations were prepared by dissolving the reagent in deionized water (Elix3-MILLIPORE®). In all cases, the synthetic influent used in the photo-catalytic experiments consisted of a mixture of the three dyes (100 mg/L each). The dye mixture (300 mg/L) was prepared from stock solutions and then diluted with tap water to reach the desired concentration.

2.2. Analytical determinations

The percentage of decolorization of the dye mixture was assessed on the basis of changes in absorbance at λ_{max}: 506 nm, using an UV–vis spectrophotometer (Perkin-Elmer UV-25, USA). Prior to UV–visible analysis, the samples were removed from the photo-reactor and quenched with a methanol–water solution (methanol: 200 mM) to prevent further degradation.

For HPLC, DOC, toxicity, biodegradability and GC/MS analyses the samples were treated with a NaOH–$Na_2S_2O_3$ solution in order to remove residual peroxide and to prevent further oxidation. The identification of intermediate products was performed by combining a dispersive liquid–liquid micro-extraction (DLLME) technique with GC/MS [25]. In the DLLME method, 0.50 mL of methanol and 0.50 mL of dichloroethane were rapidly injected by syringe into a 5 mL pre-treated sample containing the analyte, thereby forming a cloudy solution. After phase separation by centrifugation (2 min at 4000 rpm), the enriched analyte in the settled phase was analyzed by GC/MS. The GC/MS (HP 6890N and 5975, USA) was equipped with a column (HP 5MS, 30 m × 0.25 mm × 0.25 μm). The GC/MS analyses were carried out according to [26] in a splitless mode using helium as carrier gas (1 mL/min measured at 150 °C). The injector temperature was maintained at 250 °C and the oven temperature was programed as follows 40 °C for 5 min, 40–290 °C (at 12 °C/min), and then held at 290 °C for 3 min and finally 290–325 °C (at 20 °C/min), and then held at 325 °C for 5 min.

Carbon removal was monitored by measuring the DOC (dissolved organic carbon) by injecting filtered samples (Whatman-GFA) into a Shimazu-5050A TOC Analyzer (Japan). Carboxylic acids were identified using reverse-phase liquid chromatography (20 μL, flow 1 mL/min, mobile phase: potassium phosphate, pH: 2.5, 40 °C) with a diode array detector (DAD G1315A) in an HPLC-UV (Agilent Technologies 1100) with a C-18 column (Grace Prevail Organic 5 μm, 250 μm × 4.6 μm).

The H_2O_2 concentration was determined by the ammonium-metavanadate (NH_4VO_3) spectrophotometric method at 454 nm [27]. Total dissolved solids (TDS) and total solids (TS) were measured according to Standard Methods [28]. Because a large number of benzene and naphthalene compounds are expected from the degradation of the dye mixture, the Specific Ultraviolet Absorption index (SUVA) was used as a surrogate measure for the aromatic content of the photo-treated effluent [29,30]. Accordingly, the UV absorbance at 254 nm divided by the DOC was reported as the SUVA index (SUVA = UV absorbance at 254 nm/DOC).

2.3. Toxicity assays

The Microtox® toxicity assays were carried out with *Vibrio fischeri* (Microtox® Azure Environmental) according to the basic test using a SDI M500 Analyzer (Strategic Diagnostics Inc., USA). Toxicity was determined after 15 min of incubation using MicrotoxOmni software (USA) as described in the Microtox® manual [31]. Phenol was used as the reference compound in the toxicity assays (100 mg/L phenol; TU = 3; EC_{50} = 23 mg/L), which were performed within 48 h after photo-treatment to obtain the EC_{50} value. Toxicity was expressed in toxicity units (TU), where TU = 100/EC_{50}.

2.4. Biodegradability assays

The biodegradability assay (Zahn–Wellens test) was performed according to OECD protocol [32] in 0.75-L-flasks aerated by diffused air. The inoculum was obtained from an activated sludge treatment plant in Querétaro (Mexico). The Zahn–Wellens assay was initiated and then monitored for 28 days in reactors that were maintained at 28 ± 2 °C. The samples were withdrawn and centrifuged at 3000 rpm for 5 min; subsequently, the DOC of the supernatant liquid was analyzed. DOC removal was used to quantify de biodegradability of the photo-treated samples. The biodegradability percentage at time t was evaluated by means of Eq. (5), where C_A is DOC of the photo-treated azo dye mixture (measured at 3 h after the beginning of the test, mg/L), C_t is the DOC of the test mixture at time t, C_B is the DOC of the blank at time t, and C_{BA} is the DOC of the blank (measured 3 h after the beginning of the test).

$$\text{Biodegradability percentage} = \left[1 - \frac{C_t - C_B}{C_A - C_{BA}}\right] \times 100 \qquad (5)$$

Table 1
Reagent injection strategies tested: experimental design.

E_1					E_2		E_3		
Dose (%)	H_2O_2 (mg/L)	mg H_2O_2 (mg dye)	Fe^{2+} (mg/L)	mg Fe^{2+} (mg dye)	Dose (%)	Injection time (min)	Dose (%)	Flow H_2O_2 (mg/min)	Flow Fe^{2+} (mg/min)
100	400	1.33	20	0.066	100	60	100	16.6	0.83
80	320	1.06	16	0.053	80	48	80	13.3	0.66
60	240	0.798	12	0.039	60	36	60	10.0	0.50
40	160	0.532	8	0.026	40	24	40	6.66	0.33
20	80	0.266	4	0.013	20	12	20	3.33	0.16
10	40	0.133	2	0.007	–	–	–	–	–
5	20	0.067	1	0.003	–	–	–	–	–

2.5. Experimental setup

The photo-treatment experiments were carried out in a CPC (compound parabolic concentrator) solar-based reactor with a total volume of 2.5 L. The experimental setup (Fig. 1) consisted of a stirred tank (1 L), a solar collector with 0.25 m^2 and a concentration factor of 1.06 made of three pyrex-glass tubes (OD: 30 mm, ID: 28.5 mm, length: 92 cm) and a centrifugal recirculation pump. The reagent supply (Fe^{2+}–H_2O_2) was channelled through two peristaltic pumps (Masterflex) with speed control. Incident radiation (W/m^2) was measured every minute with a pyranometer (Davis Instruments Vantage Pro2^{TM}, spectral range 300–1100 nm). The reactor was fixed in an aluminum frame tilted at 20° in Querétaro (Mexico). The experiments were carried out following a fixed schedule span that extended from 11:00 AM to 3:00 PM, when the highest irradiation was present. In photo-Fenton experiments temperature evolves freely (between 28 ± 2 °C and 41 ± 4 °C) during treatment. Comparisons between the experiments were always conducted under similar irradiation conditions in order to reduce the effect of temperature and irradiation on process performance. Therefore, only those experiments that showed minor variations in accumulated energy per unit of volume (less than 10% ∼45 kJ/L) were considered for this study.

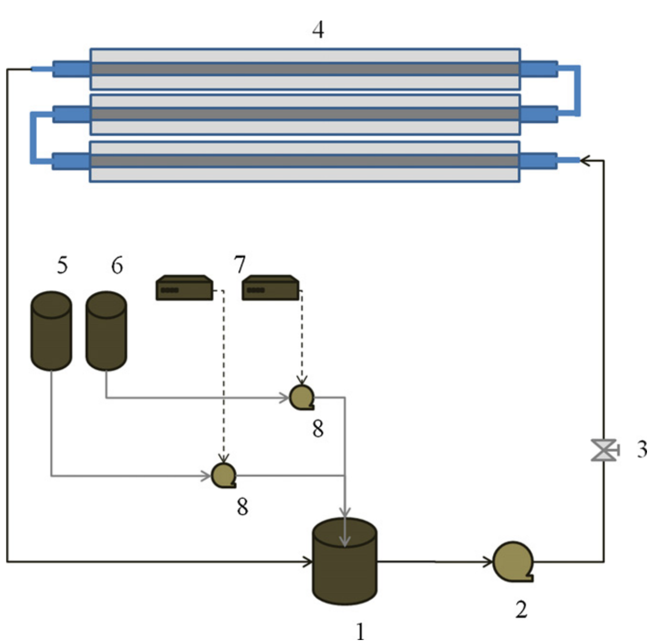

Fig. 1. CPC reactor: experimental setup. (1) Stirred tank, (2) recirculation pump, (3) valve, (4) solar collector, (5) peroxide tank, (6) iron tank, (7) speed controls, and (8) peristaltic pumps to reagent injection.

2.6. Reagent dosing strategies

The effect of three reagent dosing strategies on the percentage of decolorization, toxicity and biodegradability were tested in the CPC solar-based reactor. All experiments were conducted at the initial pH of 2.8–3.0, which is considered as the best pH for photo-Fenton oxidation [2–4]. In all cases, pH evolved freely along the photo-treatment (from 2.8 to 2.5). As indicated in a previous study [33], a central composite design (CCD) was applied to determine the reagent dose for maximizing the decolorization of AO7, AR151 and AB113 through a photo-Fenton process.

The first strategy (E_1) administered the Fenton reagent at the beginning of the test. In this strategy, the Fe^{2+} was injected into the stirred tank and then the H_2O_2 was supplied in less than 15 s (Table 1). The dosage at 100% corresponds to the amount of reagents required to decolorize 97% of the mixture of azo dyes. This condition was previously determined as 1.3 mg H_2O_2/mg dye and 0.06 mg Fe^{2+}/mg dye [33].

For the second and third strategies (E_2 and E_3), the reactants were dosed continuously using peristaltic pumps at a flow rate of 2 ± 0.2 mL/min. In the E_2 strategy the reactants were dosed continuously (16.66 mg H_2O_2/min and 0.83 mg Fe^{2+}/min), but the duration of the injection time varied, as did the amount of the reactants. In the E_2 strategy, five injection times (12, 24, 36, 48 and 60 min) were evaluated. After injection, the pumps were turned off, but the photo-treatment continued until 60 min of irradiation were completed (∼500 kJ/L of accumulated energy). Thus, in the E_2 strategy a fraction of the pre-treatment time was performed in the absence of reagents in order to take advantage of the solar-driven reactions to decolorize the dye mixture.

In the E_3 strategy, the reactants were dosed during 60 min at a constant rate, but with different solution concentrations in order to obtain the desired mass flows (Table 1). E_2 and E_3 strategies were the same at 100% of the reagent dose. In contrast to other studies [17–22], where only peroxide was added continuously to minimize the adverse reactions, in E_2 and E_3 strategies iron and peroxide were supplied simultaneously in order to minimize the extension of the Eqs. (2) and (3). The photo-Fenton experiments were performed in duplicate. The dilution caused by the continuous addition of the Fenton reagent was considered during decolorization and carbon removal analyses. Blank tests were carried out with no Fenton reagent to evaluate the effect of solar radiation on the percentage of decolorization. No appreciable decolorization was noted after 240 min (about 2000 kJ/L) of photo-treatment.

To evaluate the effect of the chemical dosage on the decolorization process, the efficiency of reactant consumption was computed (Eq. (6)). In Eq. (6), $\Delta_{\text{Absorbance}}$ represents the change in the absorbance of the solution due to a specific consumption of the Fenton's reagent (ΔH_2O_2).

$$\text{Efficiency of reactant consumption} = \left(\frac{\Delta\text{Absorbance}}{\Delta[H_2O_2]}\right) \quad (6)$$

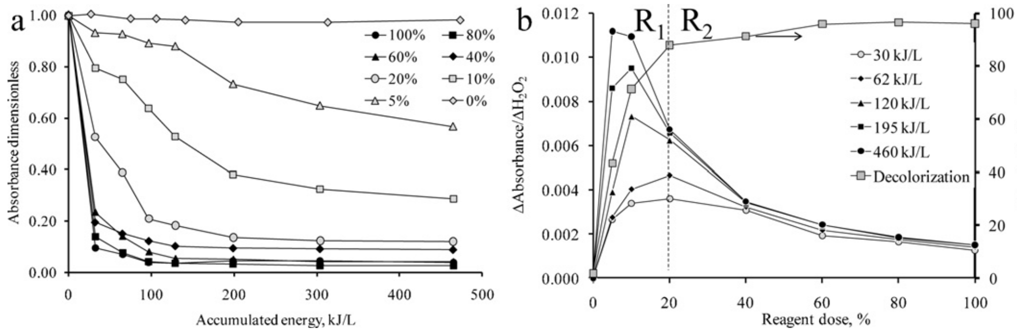

Fig. 2. Effect of the reagent dose in E_1 strategy: (a) decolorization percentage at 506 nm and (b) reactant consumption.

3. Results and discussion

The use of coupled processes for the degradation of recalcitrant substances is frequently employed to improve the robustness of a treatment system [1,11–14]. Improving the biodegradability of an azo dye mixture can be reached satisfactorily through a photo-Fenton process [1,33]; nevertheless the operative costs rise and represent an important drawback of techniques designed to degrade colored wastewaters. Therefore, the basic idea that led us to test different dosage strategies of the Fenton's reagent was to avoid undesirable reactions (see Eqs. (2)–(4)) in the process and so reduce the amount of reactants used in the decolorization step.

3.1. Reagent injection strategies: effect on the percentage of decolorization

The effect of the dosage of reagents (E_1 strategy) on decolorization is shown in Fig. 2a. With regards to the case in which no reagents were dosed (0%, Fig. 2a), it is clear that dye photolysis (Eqs. (7)–(9)) contributed only slightly to the percentage of decolorization, since less than 2% of decolorization was found after 60 min of photo-treatment (450 ± 17 kJ/L of accumulated energy). Meanwhile, more than 90% of decolorization was obtained when the reagent dose was between 20% and 100%. It is important to note that 100% represents the Fenton's reagent dose (1.3 mg H_2O_2/mg dye and 0.06 mg Fe^{2+}/mg dye) required to decolorize 97% of the dye mixture.

Lower doses of Fenton's reagent (5% and 10%) led to a reduction of the undesired reactions (Eqs. (2)–(4)) due to the lower concentrations of $HO^\bullet$ radicals present. By means of the E_1 strategy (Fig. 2a), it became feasible to achieve 43% decolorization by using 5% of the reagent dose (Table 1). In all cases, no peroxide was detected after 15 min of photo-treatment (accumulated energy: 100 ± 11 kJ/L); thus, the decolorization may be attributed to alternative pathways for iron regeneration and the production of $HO^\bullet$ radicals, such as photo-reduction of the catalyst (Eq. (9)). Also, it has been shown [2,4,34–36] that the presence of quinone–hydroquinone moieties promoted the regeneration of the catalyst by successive one-e$^-$ transfer steps via the semiquinone radical (Eqs. (11)–(13)) and the photo-reduction of quinones to semiquinones (Eq. (14)), which can produce additional $HO^\bullet$ radicals [2,4].

$$\text{Dye} + h\nu \rightarrow \text{dye}^* \quad (7)$$

$$\text{Dye}^* + h\nu \rightarrow \text{dye} \quad (8)$$

$$\text{Dye}^* + h\nu \rightarrow \text{by-products} \quad (9)$$

$$\text{Fe(OH)}^{2+} + h\nu \rightarrow \text{Fe}^{2+} + \text{H}^\bullet \quad (10)$$

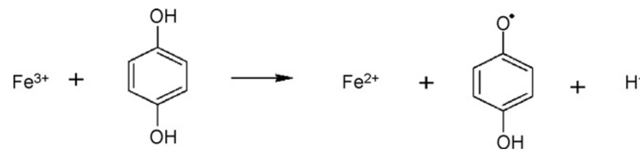

(11)

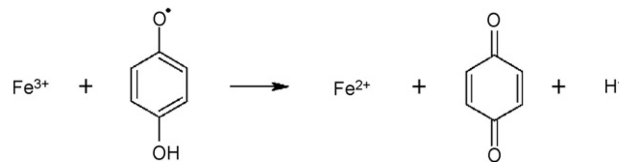

(12)

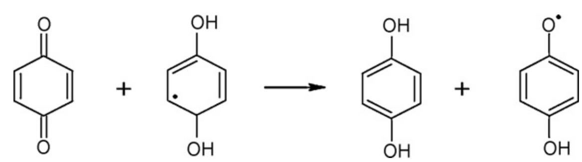

(13)

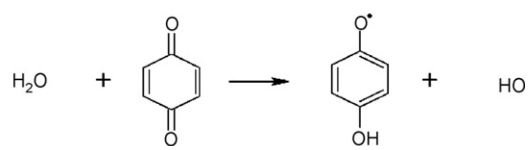

(14)

In Fig. 2b, the efficiency of reactant consumption ($\Delta_{\text{Absorbance}}/\Delta[H_2O_2]$) indicates the presence of an operative region where alternative pathways may be present and play an important role in the decolorization (R_1). In this region, lower doses of reagent were applied (from 5% to 20%) and decolorization was most likely carried out by the reductive regeneration of the catalyst through aromatic moieties and by solar photo-assisted reactions (see Eqs. (7)–(14)). Observations showed that SUVA was not removed (Table 2) when the lower doses of reagents were used. This suggests a minor transformation of the original dye's structure and the presence of quinone–hydroquinone moieties which can be used to accelerate the decolorization process [34–36]. Although the aromatic moieties may enhance decolorization and reduce operative costs, the presence of less transformed species may lead to the inhibition of a biological post-treatment process [9,10,14,16].

Table 2
General performance of the studied strategies related to SUVA index removal.

Reagent supplied as percentage	SUVA removal (%)		
	E_1	E_2	E_3
20	0.0	0.0	0.0
40	2.2	2.0	7.3
60	7.9	7.7	10.4
80	13.6	16.6	19.9
100	29.6	33.7	34.2

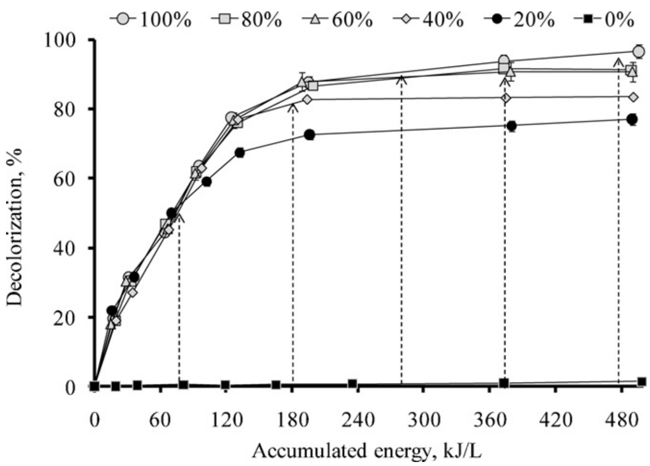

Fig. 3. Effect of the reagent dose in E_2 strategy. *Note*: The dotted lines mark the end of the reagent injection for each concentration.

A second region (R_2) where the higher doses of reagents were injected (40,60,80 and 100%) evidenced both a sharp decolorization and SUVA removal (Fig. 2b and Table 2, respectively). In this region, decolorization was accomplished by using 62 kJ/L of accumulated energy or10 min. A further irradiation (up to 450 kJ/L or 60 min) did not affected significantly the decolorization as shown in Fig. 2a and b. This can be explained because as the reagent's concentration increased, the further degradation of the dyes leads to the formation of non-aromatic compounds which cannot promote the catalyst regeneration [34–36].

The E_2 strategy was studied in order to reduce the impact of radical scavenging, as well as to take advantage of solar-driven reactions and intermediate degradation products to reduce reagent consumption. Here, the reactants were dosed continuously (16.66 mg H_2O_2/min and 0.83 mg Fe^{2+}/min), but the duration of the injection time varied (Table 1), as did the amount of reactants injected. Fig. 3 shows that 20% of the reagent dose (0.266 mg H_2O_2/mg dye and 0.013 mg Fe^{2+}/mg dye) is sufficient to decolorize up to 52% of the dye mixture in 12 min (75 kJ/L of accumulated energy), point at which the feeding pump was stopped. However an additional decolorization (up to 77%) was observed probably due to the regeneration of the catalyst by photo-reduction (Eq. (10)) and successive electron transfers steps (Eq. (11)–(14)). Furthermore, in the dark, 86% of decolorization of the same azo dye mixture was observed. But in this case 100% of the reactive dose was used [33]. This last finding indicates the important role of alternative pathways in decolorization.

As the reagent concentration increased from 40% to 100%, the impact of the alternative routes of decolorization appeared to decrease. Despite the additional reagents were supplied, the decolorization obtained after 24 min (180 kJ/L) was about 87%. This may be related to the transformation of quinone–hydroquinone moieties into short-chain acids that are recalcitrant to the HO• radicals [2–4]. The latter was confirmed by the data shown in Table 2, where an appreciable removal of SUVA was obtained when the reagent dose was increased from 20% to 100%.

Considering previous results, the reactants were injected during 60 min at a constant rate, but in different concentrations (E_3 strategy, Table 1). A dose of 60% was found to be adequate to decolorize more than 90% of the dyes (Fig. 4a). In this case, about 10% of the SUVA was removed (Fig. 4a), which indicates a slight improvement over the E_1 and E_2 strategies (Table 2). Fig. 4a shows an increase of the reagent dose in the E_3 strategy (from 60% to 100%) allowed a marginal increase in the percentage of decolorization (less than 6%); however, SUVA removal increased significantly (from 10% to 34%) due to the increase in the reagent concentration. This study aimed to maximize decolorization in order to transform the azo dyes into more biodegradable and less toxic structures, and avoid the total mineralization of the organic matter.

To further investigate the behavior of the decolorization process by means of the E_1 and E_3 strategies, the evolution of the decolorization at three absorption wavelengths (254, 310 and 506 nm) was followed using the 100% condition. Results showed that the decolorization process takes place in two steps (Fig. 4b). In the first, cleavage of the azo bond occurs, since decolorization proceeds as indicated by the reduction in the absorbance at 506 nm (section A). Next, after 110 kJ/L, the reduction of aromatic compounds (measured at 254 and 310 nm) began (section B). In the E_3 strategy, the hydroxylation process is continuous during photo-treatment due to the presence of Fenton's reagent. On the other hand, in the E_1 strategy, the extensive generation of HO• radicals allowed a rapid azo bond cleavage as well as the hydroxylation of the aromatic ring (less than 62 kJ/L). Once the reagents have been consumed the degradation process is controlled by the regeneration of the catalyst (Eq. (10)), which is considered the rate-limiting step in photo-Fenton processes [2,4]. This last fact may explain the slower decrease of absorbance at 254 and 310 nm observed in the E_1 strategy.

Color removal by the three strategies was compared using the higher doses of reagents (60%, 80% and 100%, Fig. 5a). Above 90% of final decolorization was achieved after 60 min of photo-treatment, and no significant difference (less than 4%) among the three strategies tested was observed. When the lowest reagent dose (20%) was used, significant differences on the percentages of decolorization were found; for example, by means of E_1 it is possible to decolorize 87 ± 1.9% of the mixture, whereas the E_2 and E_3 strategies allowed decolorization percentages of 77 ± 2.1% and 68 ± 1.6%, respectively.

The decolorization rate was evaluated considering a first order kinetics (Eq. (15)). In this equation, k_{app} is the apparent rate

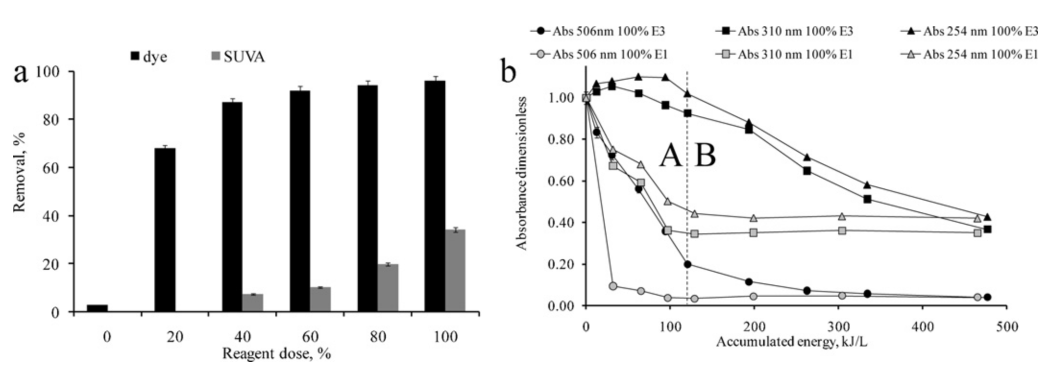

Fig. 4. Decolorization of the azo dye mixture. (a) Decolorization (506 nm) and SUVA index removal (E_3 strategy); and (b) degradation profiles of the mixture of azo dyes using the 100% dose of the Fenton's reactants for E_1 and E_3 strategies.

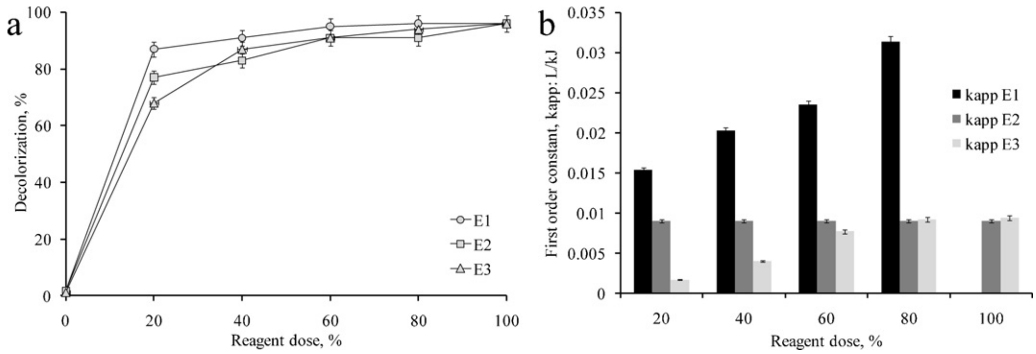

Fig. 5. General performance of the photo-treatment process. (a) Decolorization profiles and (b) Decolorization rate.

constant, E_n is the accumulated energy in kJ/L, and A_0 and A are the initial and final absorbance values of the dye mixture, respectively.

$$\mathrm{Ln}(A) = \ln(A_0) - k_{\mathrm{app}} \times E_{\mathrm{n}} \tag{15}$$

Strategy E_1 showed the highest decolorization rates, which may be related to the presence of high concentrations of the reagents (Fig. 5b). The first order model for E_1 at 100% did not fit because 90% of decolorization was carried out in fewer than 5 min (32 kJ/L), and it was not possible to obtain off-line data at this interval. The E_3 strategy presented the lowest decolorization rates, considering that the reagents were present at lower concentrations. Although the effect of reagent concentration was evident in the E_2 strategy, this behavior was notable at the lower reagent doses (20–40%). When the concentration of reagents was increased to 100%, there was no significant difference in the decolorization rates for the E_2 and E_3 strategies.

Marginal differences in the SUVA index (around 2%) were found when the results of the three strategies, at the same dose of reagents, were compared (Table 2). Chidambara and Quen [24] concluded that the addition of the same dose of reagents, in multiple steps or in a continuous mode, had a negative effect with regards to DOC removal, oxygen uptake rate and BOD improvement. On the other hand, Monteagudo et al. [22] showed that the continuous addition of peroxide positively affects the reaction rate and DOC removal of the azo dye AO7. These authors found that the same decolorization percentages can be attained with, and without, the continuous addition of reagents, but with different reaction rates; findings that agree with the results obtained in the present study. As the percentage of decolorization was unaffected by the reagent injection strategy, it was necessary to test additional parameters in order to select the best condition.

3.2. Toxicity and biodegradability assays

Supplying lower doses of reagents (40%, 60% and 80%) in the three strategies studied resulted in decolorization percentages comparable to those obtained by using 100% of the reagent dose. Therefore, in order to select the best strategy for the dosage of the reagents it was necessary to assess the effect of different reagent doses on parameters such as toxicity and biodegradability.

The toxicity assay makes it possible to determine the effluent's characteristics, whereas biodegradability assays allow researchers to evaluate the behavior of the photo-treated effluent in an activated sludge treatment plant [15,37]. As the E_1 and E_3 strategies showed the largest differences in performance (Table 2), biodegradability and toxicity assays were carried out on the photo-treated effluents from these two strategies. Thus, the effect of the strategy used (E_1 and E_3) and the reagent dose supplied (60% and 100%) were evaluated. Fig. 6 indicates that both dose and the reagent supply affected the effluent quality. For both strategies, the higher dose of Fenton's reagent (100%) led to the generation of less toxic and more biodegradable by-products than the lower dose (60%). When the 100% condition was used, 70% of the biodegradation of the effluent was attained by the aerobic consortia after 28 days of incubation. It is important to note that E_3 generated less toxicity than E_1, suggesting that the reagent supply strategy is a key-issue in improving the quality of the effluent and, therefore, increasing the probability of success of a photo-Fenton–aerobic coupled process. In E_3 strategy, the continuous dosing led to a low concentration of reactants, which may reduce the impact of Eqs. (2)–(4), increasing thus the availability of $HO^{\bullet}$ radicals. Therefore, in E_3 strategy, $HO^{\bullet}$ radicals were used to preferably to hydroxylate the azo dyes. The hydroxylated compounds are considered more biodegradable by-products [38] and in consequence less toxic. The punctual injection performed in E_1 strategy led to a high initial concentration of reagents, which usually drives the formation of less powerful oxidizing species as the $HO_2^{\bullet}$ radicals. In aqueous solution the $HO_2^{\bullet}$ radical is less reactive compared to $HO^{\bullet}$ toward most organic substrates [2]. For this reason it would be feasible the formation of more biodegradable compounds through the E_3 strategy.

Fig. 6 shows that a lower reagent dose is insufficient to produce an adequate effluent for a post-treatment step. However, the reduction of toxicity and a slight improvement in biodegradability confirm the advantages of supplying the reagents in a continuous form. For instance, the injection of 60% of the reagent dose by means of the E_3 strategy (E_3: 60%) may allow the reduction of 40% of the reagent load and produce an effluent that is less toxic and slightly more biodegradable than that obtained using the E_1 strategy (E_1: 60%). It should be noted that in E_3 the continuous addition of 100% of the reagents led to the formation of poly-substituted aromatics that present absorbance peaks between 230 and 260 nm (benzene

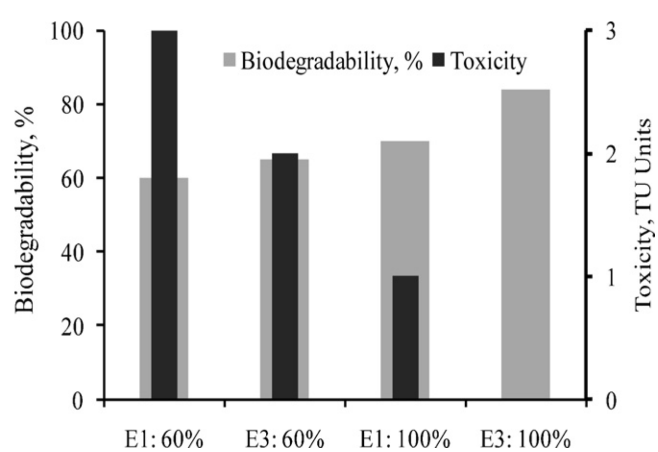

Fig. 6. Toxicity and biodegradability in E_1 and E_3 strategies after 60 min of photo-treatment.

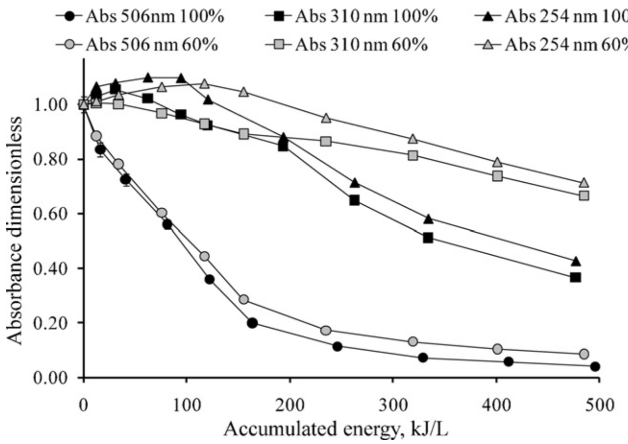

Fig. 7. Effect of the reagent dose in E_3 strategy (60% and 100%) during photo-Fenton treatment of a mixture of azo dyes.

rings) and 280 and 320 nm (naphthalene rings) as mentioned by [39–41].

The decolorization performance of the E_3 strategy was traced by measuring absorbance (254, 310 and 506 nm) for the 60% and 100% conditions. Results indicated significant differences in the aromatic content (254 and 310 nm) between the 60% and 100% doses of the reagents (Fig. 7), but no differences in decolorization behavior (506 nm) were observed. For the E_3 strategy, the 254 and 310 nm absorbance peaks increased at the beginning of the photo-treatment (0–15 min) due to the prevalence of aromatic intermediates, but the continuous reduction of absorbance reflects the rupture of the aromatic rings. This last fact suggests the transformation of the aromatic rings into more oxidized products, which are considered more biodegradable than the parent compound [3,4,13,15]. The GC/MS and HPLC analyses performed with the photo-treated effluents (E_1 and E_3 strategies) indicated that naphthol rings were further cleaved to phthalic acid and then hydroxylated to carboxylic acids such as acetic, formic, succinic, maleic and oxalic acids, all of which are highly biodegradable. Nevertheless, the supply of 60% of reagents led to the accumulation of toxic aromatic compounds (Figs. 6 and 7) that reduce the effluent quality [42,43]. Several studies have reported variable peroxide-to-iron mass-ratios (R: 2:1 to 70:1) to decolorize azo compounds [16,22,44,45]; however, in this work we observed that supplying less than 1.33 mg H_2O_2/mg dye (R: 20:1) was sufficient to decolorize a model mixture of azo dyes. Our findings show that a continuous supply of reactants contributed to reducing toxicity and improving the biodegradability of the effluent, with no increase in reagent consumption. However, long-term assays are needed in order to rule out the effect of toxicity and to ensure the robustness of the post-treatment process.

4. Conclusions

This study shows the advantages of a continuous strategy of supplying the Fenton's reagent during the degradation of an azo dye mixture. The strategies studied had no effect on the percentage of decolorization; nevertheless, it is important to note that the index of SUVA removal, toxicity reduction, and biodegradability improvement were affected by the injection strategy used and the reagent load. The best condition was the E_3 strategy, in which the reactants were dosed during 60 min at a constant rate, but with different solution concentrations. The lower reagent dose (60%) used in the E_3 strategy allowed a significant reduction of chemical consumption and generated more biodegradable intermediates. On the other hand, the higher reagent dose (100%) formed non-toxic, highly biodegradable intermediates that can be efficiently degraded in a conventional biological wastewater plant.

Acknowledgments

Financial support for this study was obtained from CONACyT (project 100298) and DGAPA-UNAM (project PAPIIT IN104710). D. Prato-Garcia acknowledged the PhD fellowship CEP-UNAM. Jaime Perez and Gloria Moreno are acknowledged for their technical assistance.

References

[1] F. Hai, K. Yamamoto, K. Fukushi, Hybrid treatment systems for dye wastewater, Crit. Rev. Environ. Sci. Technol. 37 (2007) 315–377.
[2] J. Pignatello, E. Oliveros, A. MacKay, Advanced oxidation process for organic contaminant destruction based on the Fenton reaction and related chemistry, Crit. Rev. Environ. Sci. Technol. 36 (2006) 1–84.
[3] E. Brillas, I. Sirés, M. Oturan, Electro-Fenton process and related electrochemical technologies based on Fenton's reaction chemistry, Chem. Rev. 109 (2009) 6570–6631.
[4] S. Malato, J. Blanco, W. Gernjak, Decontamination and disinfection of water by solar photocatalysis: recent overview and trends, Catal. Today 147 (2009) 1–59.
[5] Y. Dong, J. Chen, C. Li, Decoloration of three azo dyes in water by photocatalysis of Fe^{3+}–oxalate complexes/H_2O_2 in the presence of inorganic salts, Dyes Pigments 73 (2007) 261–268.
[6] S. Ergas, B. Therriault, D. Reckhow, Evaluation of water reuse technologies for the textile industry, J. Environ. Eng. 132 (2006) 315–323.
[7] X. Wang, G. Zeng, J. Zhu, Treatment of jean-wash wastewater by combined coagulation, hydrolysis/acidification and Fenton oxidation, J. Hazard. Mater. 153 (2008) 810–816.
[8] I. Arslan, T. Hanci, G. Tureli, H_2O_2/UV-C treatment of the commercially important aryl sulfonates H-, K-, J-acid and para base: assessment of photodegradation kinetics and products, Chemosphere 76 (2009) 587–594.
[9] A. Amat, A. Arques, A. Garcia, S. Malato, A reliable monitoring of the biocompatibility of an effluent along an oxidative pre-treatment by sequential bioassays and chemical analyses, Water Res. 43 (2009) 784–792.
[10] V. Sarria, S. Parra, P. Peringer, C. Pulgarín, Recent developments in the coupling of photoassisted and aerobic biological processes for the treatment of biorecalcitrant compounds, Catal. Today 76 (2002) 301–315.
[11] O. González, C. Sans, S. Esplugas, Performance of a sequencing batch biofilm reactor for the treatment of pre-oxidized sulfamethoxazole solutions, Water Res. 43 (2009) 2149–2158.
[12] T. Mandal, S. Maity, S. Datta, Advanced oxidation process and biotreatment: their roles in combined industrial wastewater treatment, Desalination 250 (2010) 87–94.
[13] J. García, F. Torrades, J. Peral, Combining photo-Fenton process with aerobic sequencing batch reactor for commercial hetero-bireactive dye removal, Appl. Catal. B 67 (2006) 86–92.
[14] A. Zapata, D. Mantzavinos, S. Malato, Scale-up strategy for a combined solar photo-Fenton/biological system for remediation of pesticide-contaminated water, Appl. Catal. B 88 (2009) 448–454.
[15] I. Oller, S. Malato, J.A. Sanchez, Combination of advanced oxidation processes and biological treatments for wastewater decontamination—a review, Sci. Total Environ. 409 (2011) 4141–4166.
[16] I. Gulkaya, G. Surucu, F. Dilek, Importance of H_2O_2/Fe^{2+} ratio in Fenton's treatment of a carpet dyeing wastewater, J. Hazard. Mater. B136 (2006) 763–769.
[17] Y. Deng, J.D. Englehardt, Treatment of landfill leachate by the Fenton process, Water Res. 40 (2006) 3683–3694.
[18] R.C. Martins, A.F. Rossi, R.M. Quinta-Ferreira, Fenton's oxidation process for phenolic wastewater remediation and biodegradability enhancement, J. Hazard. Mater. 180 (2010) 716–721.
[19] L. Prieto, I. Oller, A. Zapata, A. Aguera, S. Malato, Hydrogen peroxide automatic dosing based on dissolved oxygen concentration during solar photo-Fenton, Catal. Today 161 (2011) 247–254.
[20] J.B. Heredia, J.R. Domínguez, R. López, Advanced oxidation of cork-processing wastewater using Fenton's reagent: kinetics and stoichiometry, J. Chem. Technol. Biotechnol. 79 (2004) 407–412.
[21] O. Primo, M. Rivero, I. Ortiz, Photo-Fenton process as an efficient alternative to the treatment of landfill leachates, J. Hazard. Mater. 153 (2008) 834–842.
[22] J. Monteagudo, A. Duran, M. Aguirre, Effect of continuous addition of H_2O_2 and air injection on ferrioxalate-assisted solar photo-Fenton degradation of Orange II, Appl. Catal. B 89 (2009) 510–518.
[23] Y. Deng, Physical and oxidative removal of organics during Fenton treatment of mature municipal landfill leachate, J. Hazard. Mater. 146 (2007) 334–340.
[24] C. Chidambara, H. Quen, Advanced oxidation processes for wastewater treatment: optimization of UV/H_2O_2 process through a statistical technique, Chem. Eng. Sci. 60 (2005) 5305–5311.
[25] X. Wang, L. Fu, Y. Li, Determination of four aromatic amines in water samples using dispersive liquid–liquid microextraction combined with HPLC, J. Sep. Sci. 31 (2008) 2932–2938.

[26] EPA Method 8270, Semi-volatile organic compounds detection by gas chromatography/mass spectrometry (GC/MS).
[27] R. Nogueira, C. Oliveira, C. Parterlini, Simple and fast spectrophotometric determination of H_2O_2 in photo-Fenton reactions using metavanadate, Talanta 66 (2005) 86–91.
[28] APHA, AWWA, WPCF, in: A.D. Eaton, A.E. Clesceri, E.W. Rice, A.E. Greenberg (Eds.), Standard Methods for the Examination of Water and Wastewater, 21st ed., American Public Health Association, American Water Works Association and Water Environment Federation, Washington, D.C, 2005.
[29] A. de la Rubia, M. Rodríguez, V. León, D. Prats, Removal of natural organic matter and THM formation potential by ultra- and nanofiltration of surface water, Water Res. 42 (2008) 714–722.
[30] Metcalf, Eddy, Wastewater Engineering Treatment and Reuse, 4th ed., McGraw-Hill, New York, 2003.
[31] Azur Environmental, Microtox Manual, 1998.
[32] OECD, Guidelines for Testing of Chemicals, Degradation and Accumulation, Test No.302B: Zahn–Wellens/EVPA, 1992.
[33] D. Prato-Garcia, G. Buitrón, Degradation of azo dye mixtures through sequential hybrid systems: evaluation of three advanced oxidation processes for the pre-treatment stage, J. Photochem. Photobiol. A: Chem. 223 (2011) 103–110.
[34] J. Ma, W. Ma, W. Song, C. Chen, J. Zhao, Y. Tang, Fenton degradation of organic compounds promoted by dyes under visible irradiation, Environ. Sci. Technol. 39 (2005) 5810–5815.
[35] J. Ma, W. Ma, W. Song, C. Chen, Y. Tang, J. Zhao, Fenton degradation of organic pollutants in the presence of low-molecular-weight-organic acids: cooperative effect of quinone and visible light, Environ. Sci. Technol. 40 (2006) 618–624.
[36] F. Chen, Y. Li, L. Guo, J. Zhang, Strategies comparison of eliminating the passivation of non-aromatic intermediates in degradation of Orange II by Fe^{3+}/H_2O_2, J. Hazard. Mater. 169 (2009) 711–718.
[37] M. Lapertot, C. Pulgarín, Biodegradability assessment of several priority hazardous substances: choice, application and relevance regarding toxicity and bacterial activity, Chemosphere 65 (2006) 682–690.
[38] R. Ganesh, G. Boardman, D. Michelsen, Fate of azo dyes in sludges, Water Res. 28 (1994) 1367–1376.
[39] M. Stydili, D.I. Kondarides, X.E. Verykios, Pathways of solar light-induced photocatalytic degradation of azo dyes in aqueous TiO_2 suspensions, Appl. Catal. B 40 (2003) 271–286.
[40] W. Feng, D. Nansheng, H. Helin, Degradation mechanism of azo dye C. I. reactive red 2 by iron powder reduction and photooxidation in aqueous solutions, Chemosphere 41 (2000) 1233–1238.
[41] H.M. Pinheiro, E. Touraud, O. Thomas, Aromatic amines from azo dye reduction: status review with emphasis on direct UV spectrophotometric detection in textile industry wastewaters, Dyes Pigments 61 (2004) 121–139.
[42] A. Zapata, I. Oller, C. Sirtori, A. Rodríguez, S. Malato, Decontamination of industrial wastewater containing pesticides by combining large-scale homogeneous solar photocatalysis and biological treatment, Chem. Eng. J. 160 (2010) 447–456.
[43] C. Rodrigues, L. Madeira, R. Boaventura, Treatment of textile effluent by chemical (Fenton's reagent) and biological (sequencing batch reactor) oxidation, J. Hazard. Mater. 172 (2009) 1551–1559.
[44] N.P. Tantak, S. Chaudhari, Degradation of azo dyes by sequential Fenton's oxidation and aerobic biological treatment, J. Hazard. Mater. B136 (2006) 698–705.
[45] M. Neamtu, A. Yediler, I. Siminiceanu, A. Kettrup, Oxidation of commercial reactive azo dye aqueous solutions by the photo-Fenton and Fenton-like processes, J. Photochem. Photobiol. A 161 (2003) 87–93.